Supplementary Information

Surface state-controlled C-dots/C-dots based dual-emission fluorescent nanothermometer for intra-cellular thermometry

Chan Wang[§], Tantan Hu[§], Tiju Thomas[※], Shanliang Song[*], Zhuoqi Wen[*], Chuanxi Wang,[*] Qijun Song[*,§] and Minghui Yang[*,*]

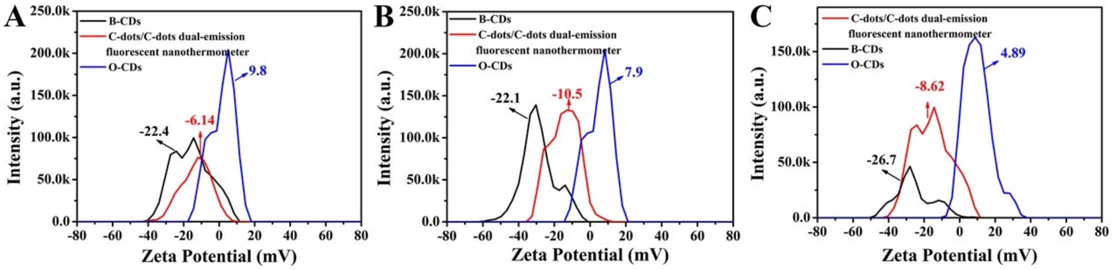

Fig S1. Zeta potential distribution of B-CDs (black line), O-CDs (blue line), and C-dots/C-dots dual-emission nanospheres (red line) at different pH, respectively. A: pH=5.0, B: pH=7.0, C: pH=9.0.

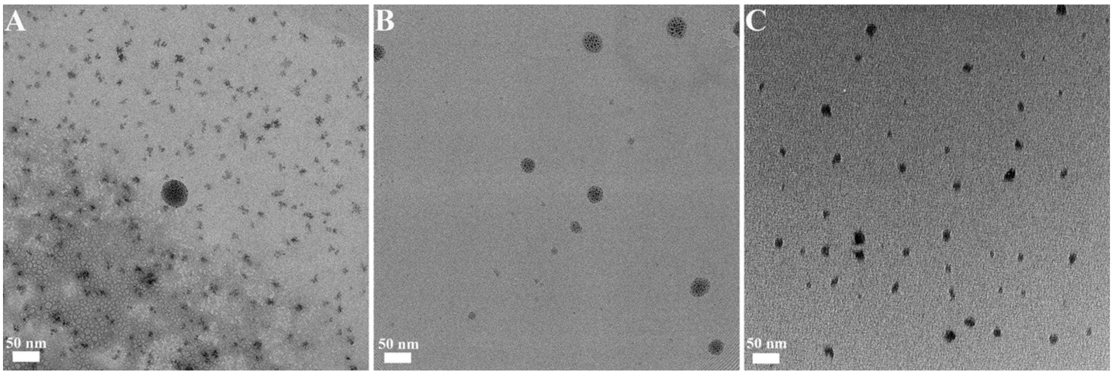

Fig S2. TEM of C-dots/C-dots dual-emission nanospheres at a varying feeding ratio of O-CDs to B-CDs: A, 3:1; B, 1:1; C, 1:2, respectively.

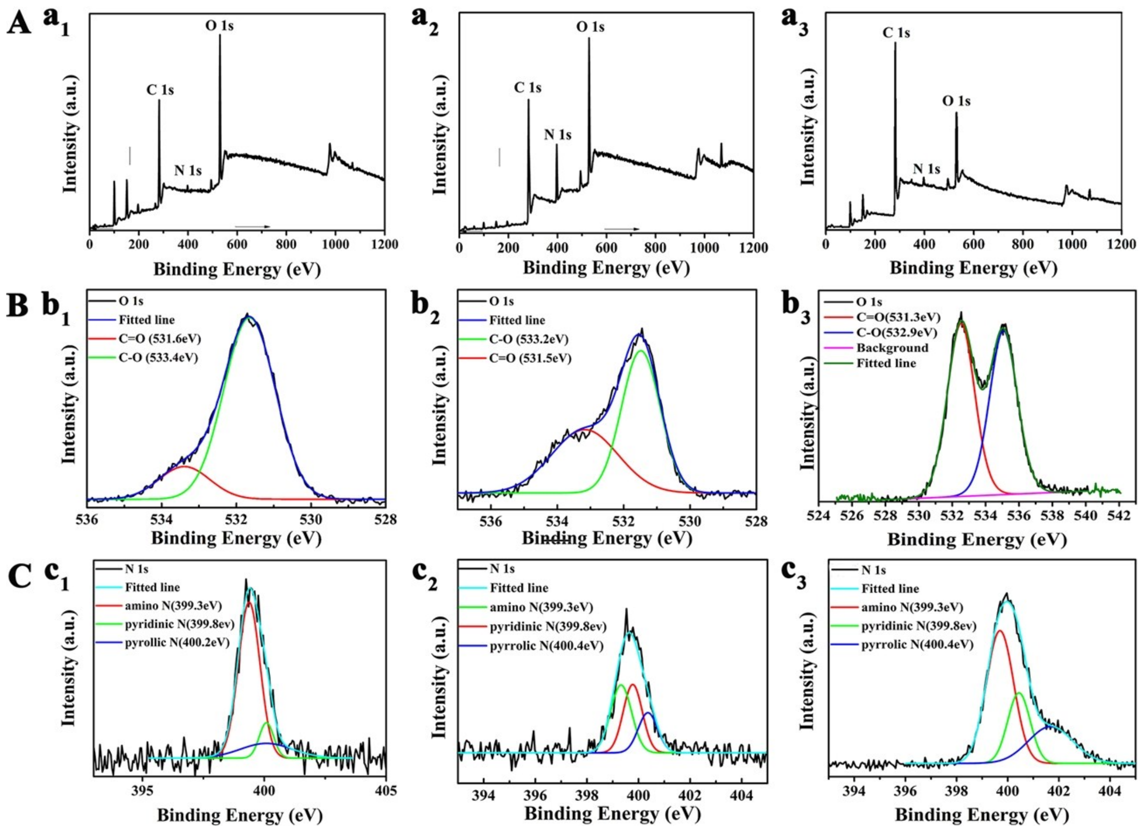

Fig S3. A: Full-survey X-ray photoelectron spectroscopy (XPS) of B-CDs (a_1), O-CDs (a_2), C-dots/C-dots dual-emission nanospheres (a_3); B: high-resolution XPS O1s spectra of B-CDs 120 (b_1), O-CDs (b_2), CDs-based dual emissive nanoparticles (b_3); C: high-resolution XPS N1s spectra of B-CDs 120 (c_1), O-CDs (c_2), CDs-based dual emissive nanoparticles (c_3). Each band was deconvoluted following the literature.

Table S1. XPS data analyses of the C 1s spectra of B-CDs, O-CDs and C-dots/C-dots dual-emission nanospheres.

Sample	C-C/C=C	C-N/C-O	C=O	COOH
B-CDs	0.404	0.313	0.255	0.028
O-CDs	0.375	0.357	0.231	0.037
C-dots/C-dots dual-emission nanospheres	0.408	0.244	0.303	0.046

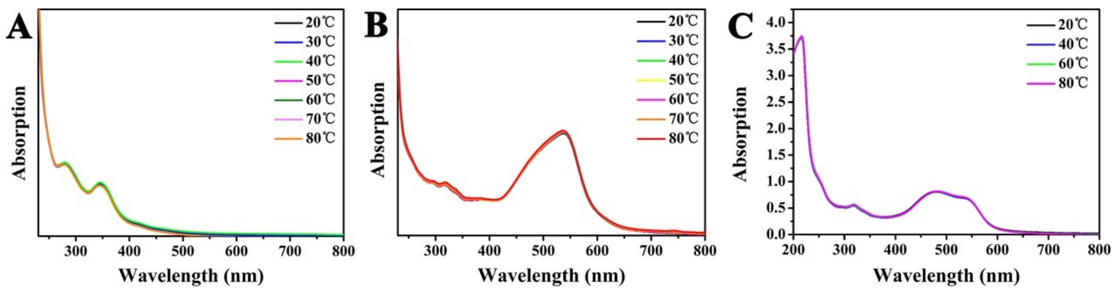

Fig S4. Absorption spectra of B-CDs (A), O-CDs (B), C-dots/C-dots dual-emission nanospheres (C) under varying temperature, respectively.

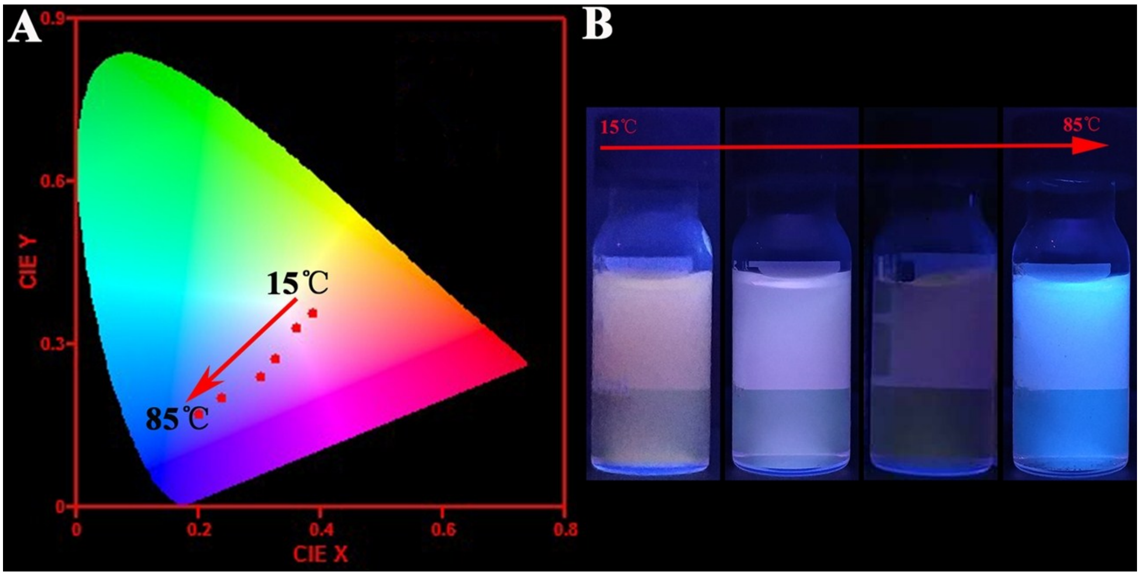

Fig S5. A: variation in the color coordinates of the C-dots/C-dots dual-emission nanospheres with increasing temperature from 15 to 85 ℃; B: corresponding photograph of the C-dots/C-dots dual-emission nanospheres under increasing temperature.

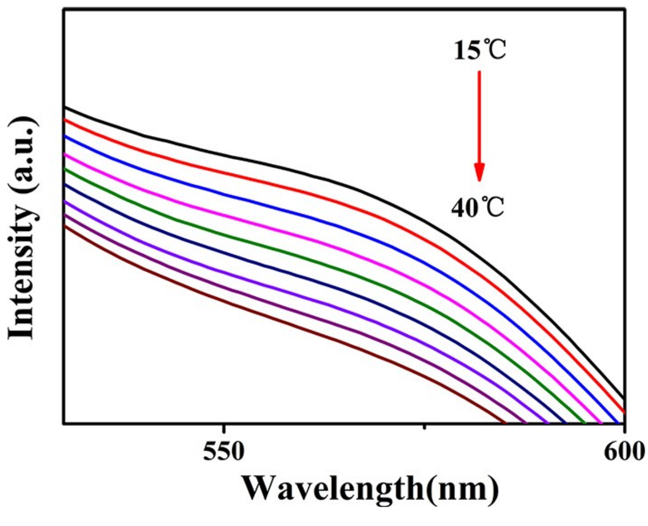

Fig S6. The magnified pattern at 590 nm of Figure 4A.

Table S2. A contrast of temperature responsive properties for recently reported CDs based nanothermometer.

Materials	Synthesis Method	Propertie	Temperature range	Sensitivity	Comment	Reference
Zn-CQDs	Zinc reduction method	single emission	10-100℃	______	Low sensitivity and poor accuracy	1
CDs	Hydrotherm-al method	single emission	15-90℃	0.69%/°C	Poor accuracy and rpeatability	2
CDs@UiO-66	In-situ synthesis	single emission	25-110℃	________	Low sensitivity and poor accuracy	3
CDs-Au NCs	Chemical crosslinking	dual emission	20-75℃	1.8%/°C	Complicated experiment procedure	4
CDs@ $(PSS/LDH)_n$ UTFs	Layer-by-lay-er assembly	dual emission	0-80℃	0.68%/°C	Cumbersome process and low sensitivity	5
MSCDs	Multi-step synthesis	dual emission	20-50℃	1.29%/°C	CDs are not temperature sensitive	6
C-dots/C-d-ots	Electrostatic self-assembly	dual emission	15-85℃	0.93%/℃	Simple, fast preparation and relatively high sensitivity	This work

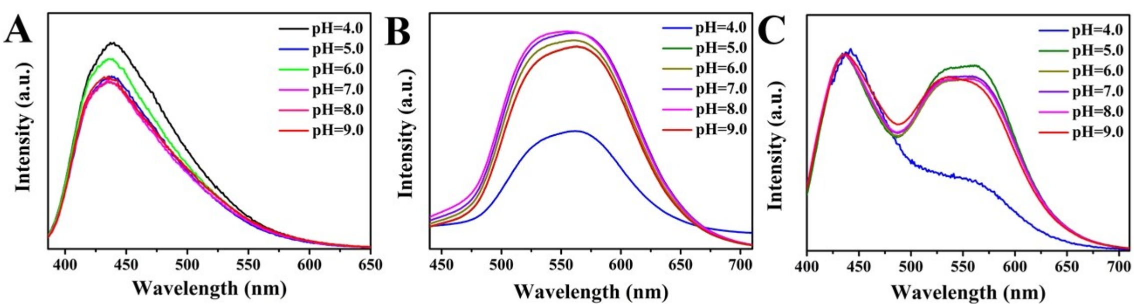

Fig S7. The PL spectra of B-CDs (A), O-CDs (B) and C-dots/C-dots dual-emission nanospheres (C) under different pH ranges (4.0-9.0).

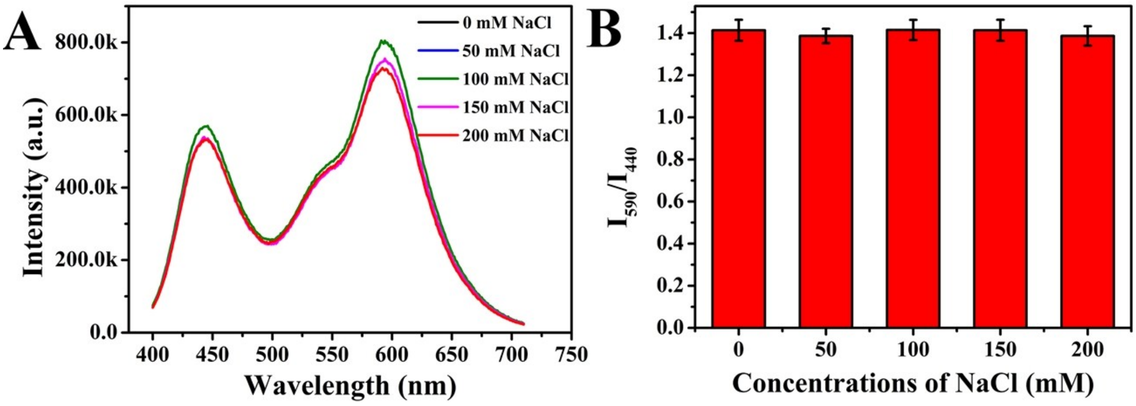

Fig S8. The PL intensity variation of C-dots/C-dots dual-emission nanospheres under different concentrations of NaCl (0-200mM).

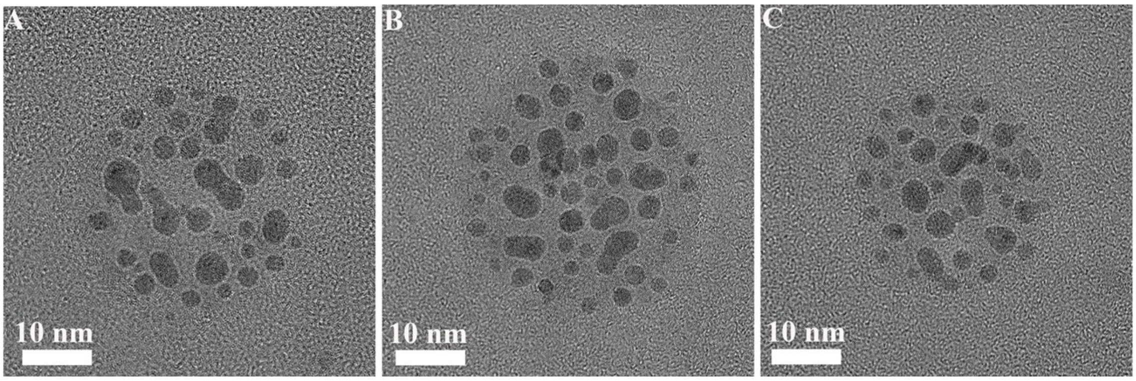

Fig S9. The HRTEM of C-dots/C-dots dual-emission nanospheres under a pH of 5.0 (A), 7.0 (B) and 9.0 (C), respectively.

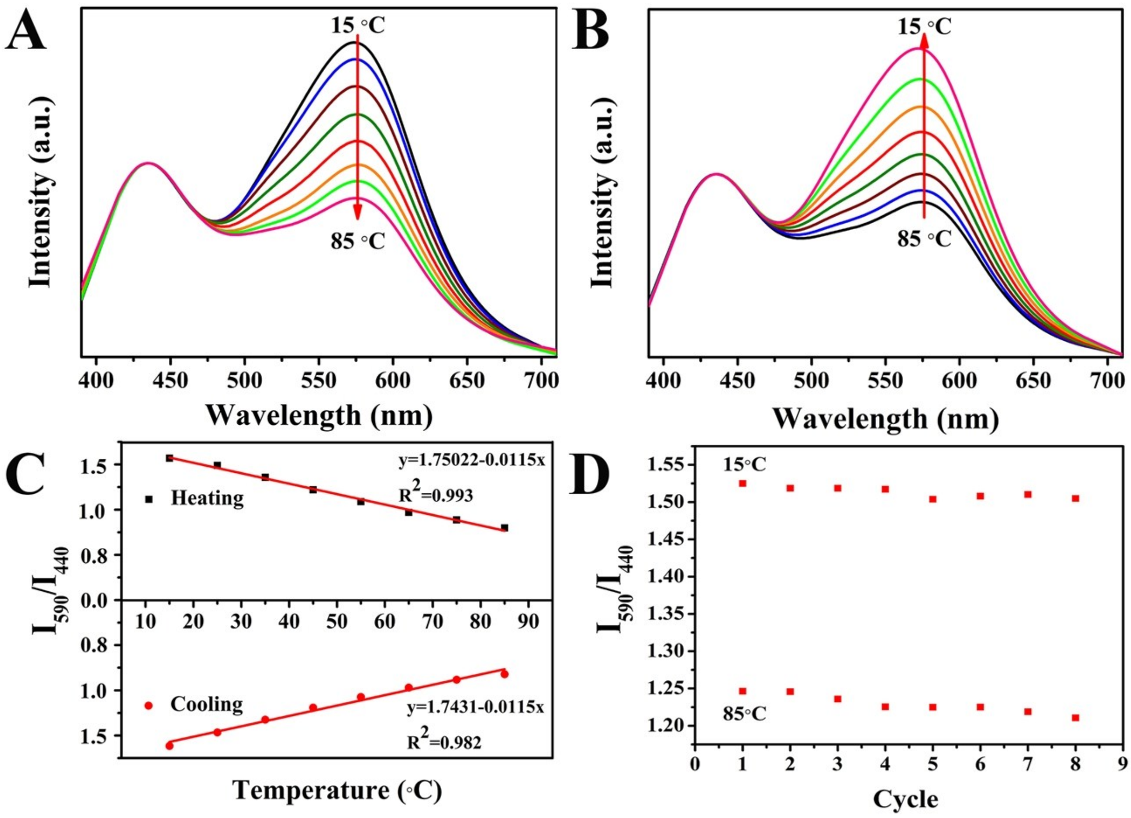

Fig. S10 Temperature dependence of the fluorescence intensity from C-dots/C-dots dual-emission nanospheres in simulated physiological solution (pH～6.5-7.0, concentration of NaCl is 200 mM). (A) Fluorescence spectra measured under excitation of 380 nm with increasing temperature from 15 to 85 oC at steps of 10 ^{o}C. (B) Fluorescence spectra (excitation 380 nm) for the decrease of temperature from 85 to 15 ^{o}C. (C) the fitted curve of intensity ratio of 440 to 590 nm vs. temperature. (D) eight cycles of intensity variations measured at 15–85 ^{o}C.

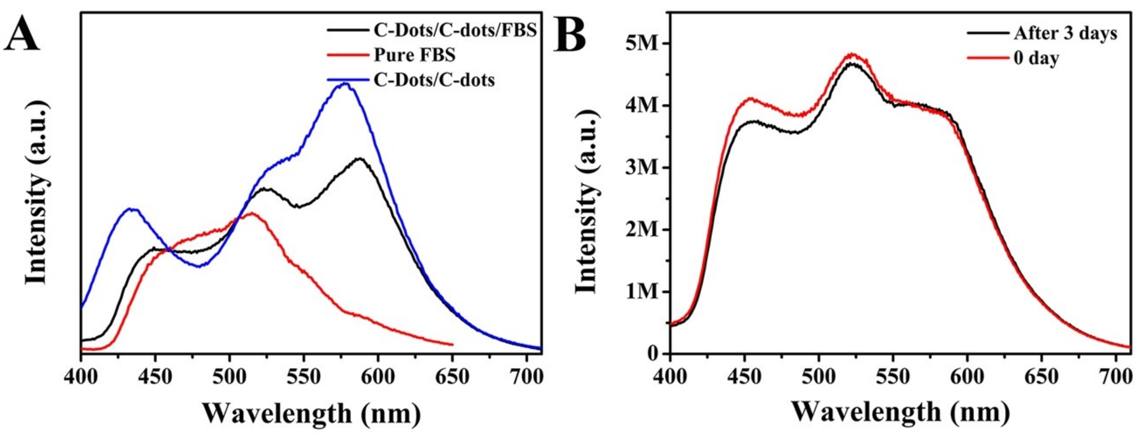

Fig. S11 A: the PL spectra of C-dots/C-dots dual-emission nanospheres (blue), pure FBS (red line), and C-dots/C-dots/FBS composites (black line); B: the PL intensity variation of C-dots/C-dots/FBS composites after placed 3 days at room temperature.

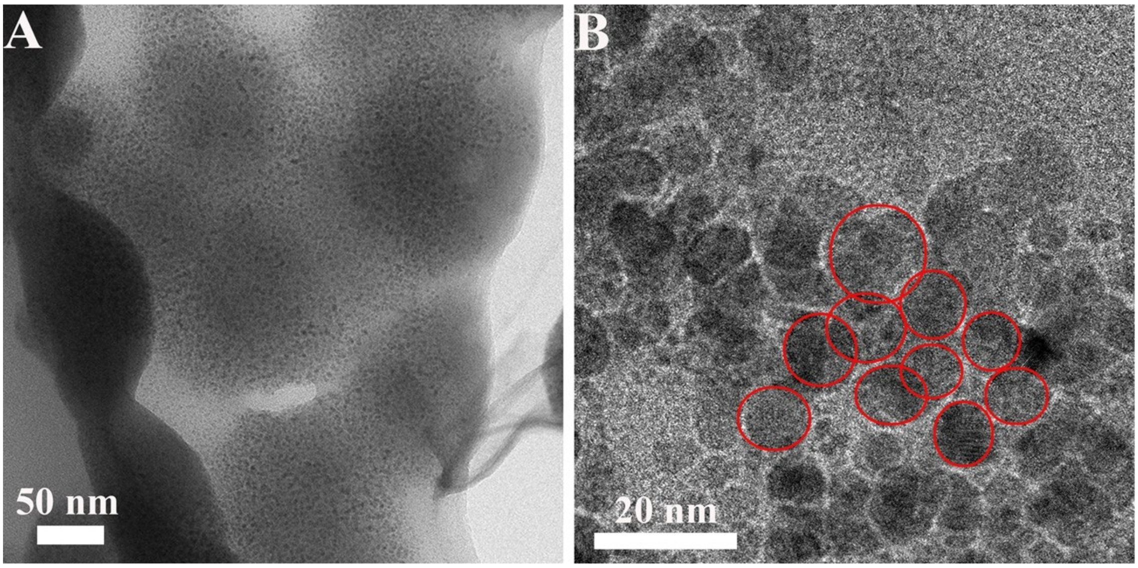

Fig. S12 The TEM and magnified images of C-dots/C-dots/FBS composites, respectively.

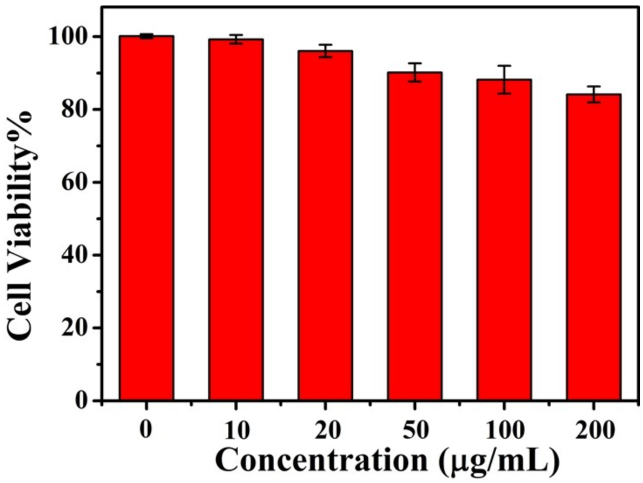

Fig S13. Cytotoxicity of the C-dots/C-dots dual-emission fluorescent nanothermometer toward of MC3T3–EI cells, as assessed using the MTT method.

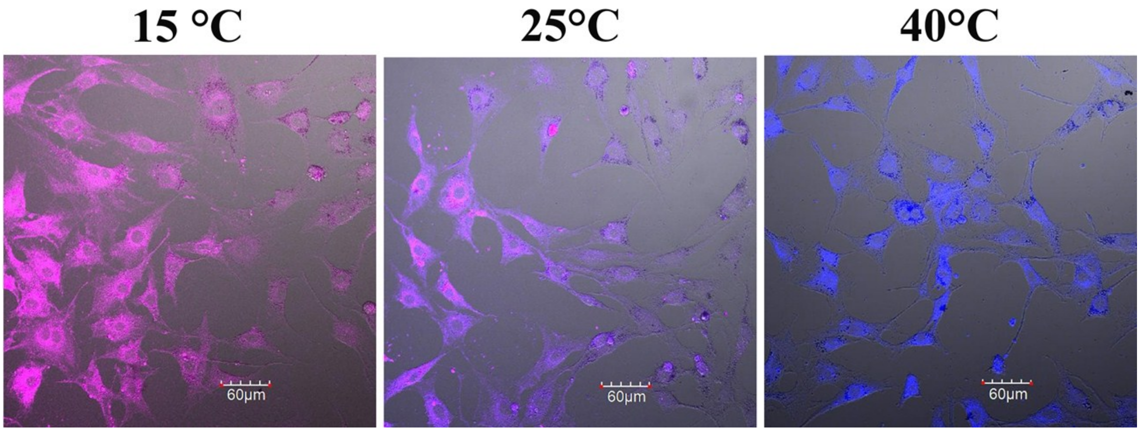

Fig S14. Confocal fluorescence images of MC3T3–EI cells under different physiological temperature, incubated with 20 μg/mL of C-dots/C-dots dual-emission nanospheres for 12 h. All images are obtained using an excitation of wavelength 405 nm. The emissions are recorded in the same range of 420–750nm.

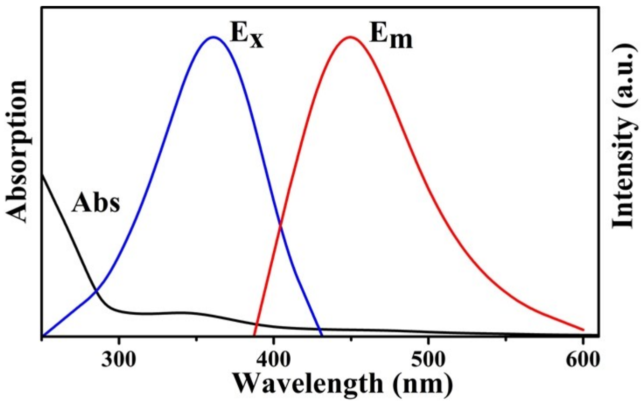

Fig S15. The absorption curves, excitation spectra and emission spectra of B-CDs.

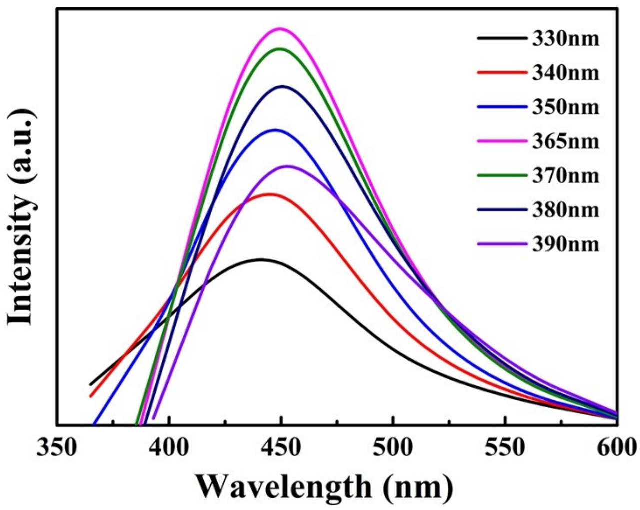

Fig S16. The PL emission spectra of B-CDs with different excitation wavelengths.

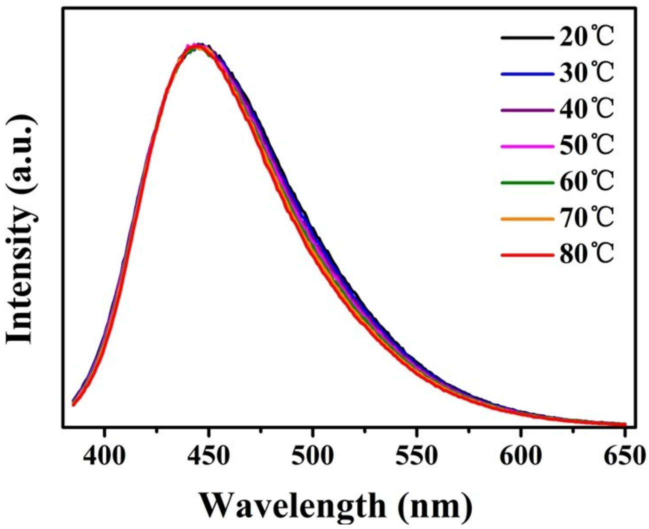

Fig S17. The PL emission spectra of B-CDs under different temperature, excited by the optimal excitation wavelength of 370nm.

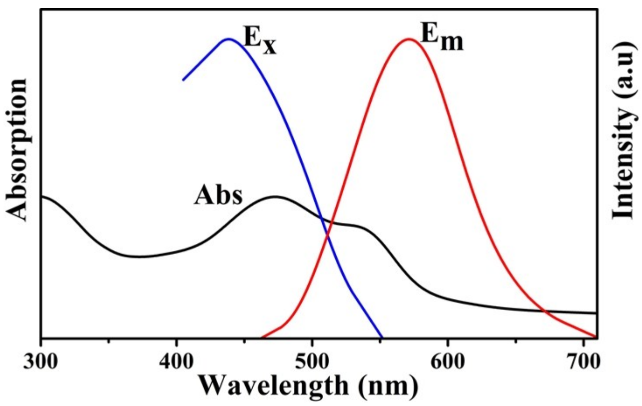

Fig S18. The absorption curves, excitation spectra and emission spectra of O-CDs.

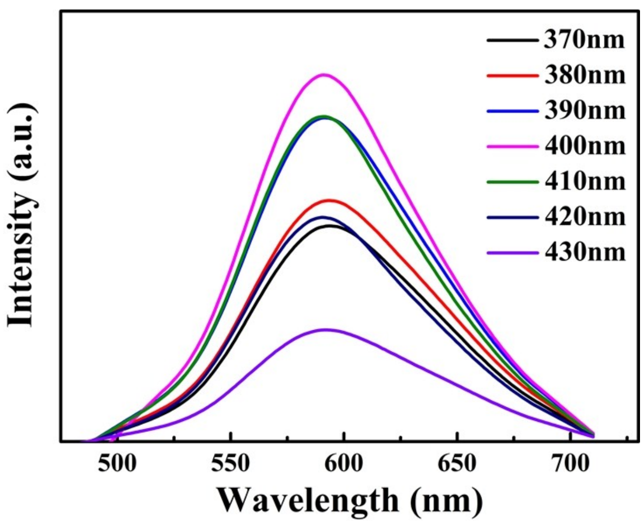

Fig S19. The PL emission spectra of O-CDs with different excitation wavelengths.

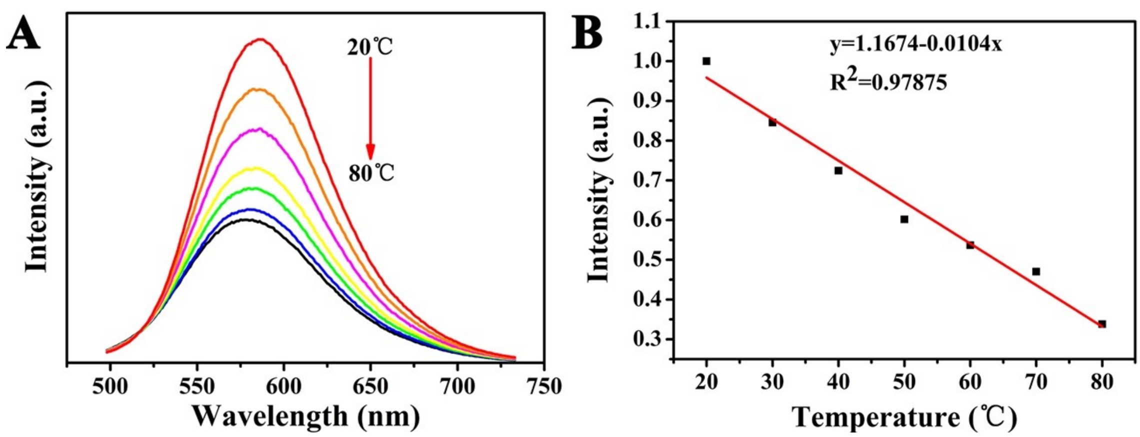

Fig S20. Temperature dependence of the fluorescence intensity from O-CDs in aqueous solution. A: Flourescence emission spectra mearused under excitation of 400 nm with the increasing temperature from 20 to 80 ℃ at a step of 10 ℃; B: the fitted curve of intensity of 585 nm vs. temperature.

Table S3. Average fluorescence lifetime of B-CDs under different temperatures.

T(℃)	τ_{ave}(ns)
20	4.9
40	5.2
60	5.1
80	5.1

Table S4. Average fluorescence lifetime of O-CDs under different temperatures.

T(℃)	τ_{ave}(ns)
20	3.8
40	3.8
60	3.7
80	3.6

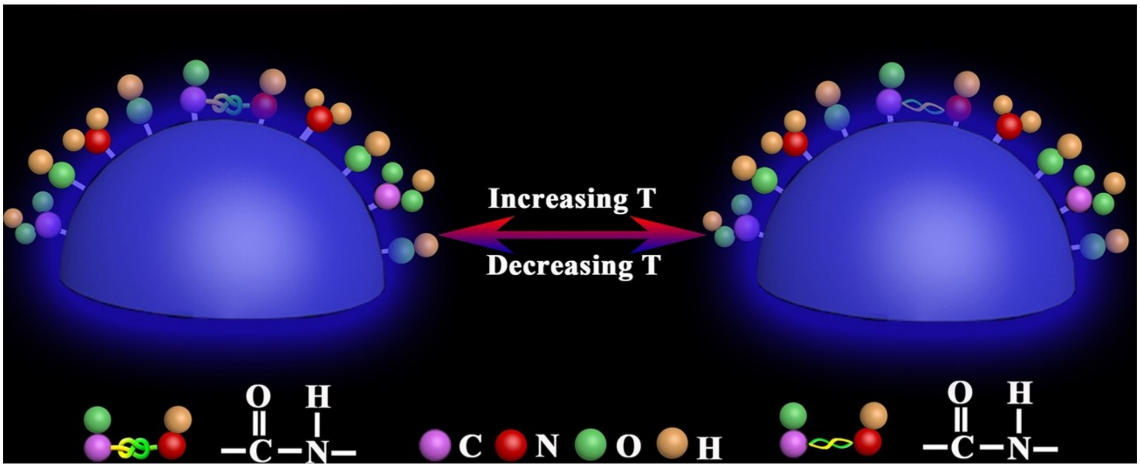

Fig S21. Scheme showing the surface state change of B-CDs.

Reference

1. R. Miao, S. Zhang, J. Liu and Y. Fang, *Chem. Mater.* 2017, **29**, 5957-5964.
2. C. Wang, Z. Xu, H. Cheng, H. Lin, M. G. Humphrey and C. Zhang, *Carbon* 2015, **82**, 87-95.
3. C. Yao, Y. Xu and Z. Xia, *J. Mater. Chem. C* 2018, **6**, 4396-4399.
4. C. X. Wang, H. H. Lin, Z. Z. Xu, Y. Huang, M. G. Humphrey and C. Zhang, *ACS Appl. Mater. Interfaces* 2016, **8,** 6621-6628.
5. W. Liu, S. Xu, Z. Li, R. Liang, M. Wei, D. G. Evans and X. Duan, *Chem. Mater.* 2016, **28**, 5426-5431.
6. X. Liu, X. Tang, Y. Hou, Q. Wu and G. Zhang, *RSC Adv.* 2015, **5**, 81713–81722.